Chain Mediation Path Optimization for Smartphone Dependence Prediction Using Graph Neural Networks and Reinforcement Learning

Guiping Xuan, Tianping Li*
Hunan Polytechnic of Environment and Biology, Hengyang, Hunan, 421000, China
E-mail：ltp0922@163.com
*Corresponding author

Keywords: Chain Mediation path, Graph modeling, Deep learning, Reinforcement learning, Causal inference

Received: Januar 22, 2026

Smartphone dependence prediction and subjective well-being impact analysis are challenged by complex variable interactions, suboptimal mediation-chain optimization, and limited interpretability. This paper proposes a chain mediation path optimization framework that formalizes mediation as a directed causal graph, where nodes denote behavioral and psychometric variables and edges encode dependency relations. Graph convolutional neural networks learn high-level node embeddings, and an attention-based multi-scale causal embedding module enhances structural expressiveness at semantic and topological levels. For path optimization, a policy-gradient reinforcement learning module dynamically updates edge weights under a reward that balances prediction accuracy, path consistency, and computational cost. A graph autoencoder with geometric consistency constraints is introduced to stabilize reconstructed mediation chains and preserve structural coherence. The framework is evaluated on 5,724 users, with an average of 58 behavioral features and 12 psychometric indicators per sample, using stratified sampling and cross-validation. The proposed model achieves 92.1%±0.4 Accuracy, 89.4%±0.6 F1-score, and 87.8%±0.5 Topology Score, outperforming a structural equation model baseline and a deep neural network without causal-path constraints. Ablation results verify that attention, reinforcement learning, and geometric constraints jointly improve classification performance and path stability. These results indicate that graph-based mediation path modeling enables unified prediction of dependence and well-being outcomes with improved interpretability and deployability in large-scale settings.

Povzetek: Prispevek predstavi grafni okvir z grafnimi nevronskimi mrežami in ojačitvenim učenjem za optimizacijo mediacijskih poti, ki natančneje napoveduje odvisnost od pametnih telefonov in njen vpliv na subjektivno dobrobit ter hkrati izboljša razlagljivost modela.

1 Introduction

The development of artificial intelligence and causal inference has driven the intelligent modeling of complex behavioral data, providing new ideas for user behavior prediction and multi-task causal representation. As a high-frequency interactive tool, the dependence behavior of smartphones is encoded by usage patterns and subjective well-being scores. However, features such as usage duration, interaction frequency, sleep patterns, and emotional states have nonlinear dependencies and causal chains, making it difficult for traditional statistical models to handle them effectively. Especially in the study of chain mediating effects, the interaction of variables presents high-dimensional, multi-level and dynamic characteristics, and it is difficult for regression and structural equation models to balance prediction and interpretation.

Existing research has provided empirical foundations for smartphone dependence modeling and user state inference. Beames et al. (2024) utilized sensor data to detect depression and anxiety in adolescents, demonstrating the value of multimodal characteristics [1]. Asare et al. (2021) proposed a depression prediction method based on machine learning and hyperparameter optimization, and combined feature importance analysis to improve accuracy [2]. Shin and Dey (2013) verified the role of behavioral data in dependency modeling by using patterns to detect problematic behaviors [3]. The MoodScope framework proposed by LiKamWa et al. (2013) realizes emotion recognition based on the use of data [4]. Stachl et al. (2020) further demonstrated the potential of smartphone data in large-scale behavior modeling and user profiling by predicting personality traits [5].

Despite this, the existing methods still have shortcomings: most studies remain at the level of feature correlation and lack structured expression at the causal chain level; The lack of a dynamic optimization and feedback mechanism for the mediating effect chain makes

it difficult to adapt to complex environments. The insufficient interpretability and scalability of the model limit its cross-scenario application.

To address these issues, this paper proposes a chain-mediated path optimization framework that abstracts the mediation process as a directed causal graph. Graph convolutional networks are used for node embedding, an attention module highlights influential mediators, and a policy-gradient reinforcement learning module dynamically updates path weights to improve both predictive performance and path consistency. A graph autoencoder with geometric-consistency constraints is further introduced to stabilize the reconstructed chains and reduce structural drift.

The research design follows three concrete goals and measurable outcomes. The first goal is to construct a computable chain-mediation graph from behavioral logs and psychometric indicators, producing a topology-aware directed graph representation. The second goal is to improve dependence and well-being prediction through GNN embeddings and multi-scale attention, evaluated by Accuracy, F1-score, and Topology Score under cross-validation. The third goal is to optimize and stabilize mediation paths via reinforcement learning and geometric constraints, validated by ablation and robustness tests.

Accordingly, this study addresses three research questions: RQ1: Can chain-mediated paths represent complex causal chains through graph modeling? RQ2: Can attention-based multi-scale representations improve mediating variable identification and path prediction? RQ3: Can reinforcement learning enhance path-weight updating while maintaining consistency between prediction and interpretation?

The innovation of this study lies in: the method formalizes the chain mediation path into a graph modeling task, integrating deep learning and causal inference to achieve structured expression; The attention mechanism is introduced in the task to form a collaborative framework with reinforcement learning, enhancing the robustness of the model under complex behavioral data. For the first time in application, chain mediation path optimization was used to model smartphone dependence and well-being, proposing an interdisciplinary and computable causal inference scheme.

2 Relevant work

In the prediction of smartphone dependence and the modeling of subjective well-being, existing research mainly focuses on three directions: application prediction, causal modeling, and path optimization. In terms of behavior and application prediction, Yu et al. (2017) established a prediction model by leveraging application usage and point of interest features, revealing the coupling effect between contextual data and behavioral patterns [6]. Yuchi et al. (2024) proposed a new user event prediction method based on causal inference, which improved the generalization performance in complex environments [7]. Kwapisz et al. (2011) utilized an acceleration sensor for activity recognition, demonstrating the feasibility of sensor data in dependent behavior modeling [8]. In the field of causal modeling and optimization, Aglietti et al. (2020) proposed a causal Bayesian optimization method for the selection of key causal variables in high-dimensional Spaces [9]. Zhang and Zhang (2024) optimized the structure of causal networks based on active learning, enhancing the efficiency of causal relationship learning [10]. Cousineau et al. (2022) conducted a review and empirical comparison of optimization-based causal effect estimation methods, clarifying the applicable scenarios of different algorithms [11]. Cao (2025) combines causal state masking with deep reinforcement learning for dynamic path planning, demonstrating adaptive optimization capabilities [12]. Mi et al. (2019) achieved real-time recognition of smartphone behavior through time series algorithms, demonstrating the value of time series modeling for dependency prediction [13]. In the field of complex systems and cross-scenario reasoning, Sun et al. (2024) utilized causal network reconstruction to achieve industrial process prediction, verifying the feasibility of causal modeling in complex systems [14]. Kalisch and Buhlmann (2014) systematically reviewed causal structure learning and inference methods, providing a theoretical basis for path optimization [15]. Hua et al. (2022) proposed a zero-shot prediction method based on causal inference, which solved the cross-scenario modeling problem in non-stationary environments [16]. Xing et al. (2024) designed a deep learning causal inference architecture for modeling the relationship between stock closing prices and related factors, demonstrating the integration potential of causal inference and deep models [17]. Gao et al. (2024) summarized the current application status of causal inference in recommendation systems, providing an important reference for multi-task prediction [18]. In the direct application of dependency prediction, Raj et al. (2024) proposed a machine learning-based addiction prediction model that effectively identified users' smartphone dependences [19]. Li et al. (2025) identified the key factors of adolescent dependence through machine learning and network analysis, providing empirical support for mediating variable modeling [20]. Boulkroune et al. (2025) presented practical finite-time fuzzy synchronization with chattering-free designs, providing a finite-time performance viewpoint that can be leveraged to discuss invariance and stability of learned paths beyond predictive gains [21].Rigatos et al. (2024) developed a flatness-based successive-loop control scheme for autonomous quadrotors, showing how structured loops can deliver explicit stability-oriented constraints that are comparable to path-level optimization objectives in data-driven frameworks [22]. Rigatos et al. (2020) further investigated nonlinear optimal control for autonomous submarines' diving, highlighting the role of convergence-aware objective design when system dynamics exhibit strong nonlinearity and external disturbances [23]. Rigatos et al. (2024) extended the successive-loop flatness-based formulation to dual-arm robotic manipulators, providing additional evidence that decomposed control paths can remain stable under coupled multi-actuator interactions [24]. Rigatos et al. (2017) reported a nonlinear optimal control method for submarine diving in industrial

electronics setting, offering a practical reference for linking optimized trajectories to enforceable control policies [25]. Zouari and Mahmud (2024) proposed a neural network-based robust adaptive output-feedback control method for MIMO time-varying delay systems, emphasizing robustness and stability considerations under time-varying uncertainties that align with distribution-shift concerns in learned mediation chains [26]. To provide a verifiable comparison between prior studies and the proposed approach, the representative methods and their datasets, modeling ideas, and reported outcome types are summarized in Table 1.

Table 1: Summary of representative related methods, reported outcome types, and limitations.

Method (Ref.)	Year	Dataset	Main approach	Reported metric / outcome type	Stated limitation
App-Predict [6]	2017	Behavior + POI data	Application behavior modeling	Classification performance (Acc)	Limited causal dependency; weak chain-level modeling
Event-Causal [7]	2024	User interaction logs	Causal inference for event prediction	Event prediction performance (F1)	Generalization under complex environments remains limited
Causal-BayesOpt [9]	2020	Synthetic causal data	Bayesian optimization + variable selection	Causal structure quality (Topology-related)	Efficiency degrades in high-dimensional causal spaces
DRL-Path [12]	2025	Path simulation environment	Causal state masking + reinforcement learning	Path planning / policy performance (Acc-type)	Limited validation on real dependence and well-being scenarios
This paper (Causal-Path GNN+RL)	2025	5,724 user data	Graph modeling + attention + RL path optimization	Acc, F1, and Topology Score (reported in this study)	Distribution-shift stability and deployment-oriented confidence reporting require further analysis

Current research remains limited in explicit chain-level causal graph modeling, feedback-driven dynamic path optimization, and robustness under scenario shifts. Therefore, a unified framework that integrates graph-based mediation representation, reinforcement learning path optimization, and feedback regulation is required to support dependable multi-task dependence prediction and well-being modeling.

3 Modeling scheme design

3.1 Chain mediation path modeling framework

The core of chain-mediated path modeling lies in transforming the causal relationship between smartphone dependence behavior and subjective well-being into a computable graph structure to support deep learning and path optimization. In this framework, variables are abstracted as nodes, causal relationships are connected in the form of edges, and paths represent the transmission logic of mediating effects. The overall form is defined as:

$$G=(V,E),\ V=\{v_1,v_2,\ldots,v_n\},\quad E\subseteq V\times V \tag{1}$$

Among them, V is a set of variable nodes, including key variables such as the duration of smartphone usage, interaction frequency, sleep patterns, emotional states, and subjective well-being; E is the causal edge set, which is used to describe the dependency relationship between variables. Each node constructs the initial feature vector $x_i \in R^d$ by extracting behavioral and psychological attributes, which is defined as:

$$F(v_i)=\left[f_t^i, f_f^i, f_s^i, f_e^i, f_c^i\right]\in R^d \tag{2}$$

Among them, f_t^i represents the usage duration feature of node i, which is used to characterize the intensity of mobile phone usage. f_f^i represents the interaction frequency feature, reflecting the level of social activity. f_s^i is a sleep pattern parameter, describing the circadian rhythm and sleep quality; f_e^i is the emotional level score, indicating the degree of social anxiety. f_c^i represents the subjective well-being score, reflecting the overall level of psychological state. This formula realizes the unified encoding of the original behavior and psychometric data, enabling them to be used as the input of graph convolutional networks, ensuring the consistency of feature scales among different samples, and providing a basis for the subsequent optimization of causal chains.

In chain path modeling, it is also necessary to introduce position embedding to quantify the relative relationship between nodes. Its calculation method is defined as:

$$P(v_i, v_j) = \frac{\left\| c_i - c_j \right\|_2}{d} \tag{3}$$

Among them, $P(v_i, v_j)$ is the relative position embedding of node i and node j, representing the structural difference between the two nodes in the causal chain; c_i, c_j are the feature center vectors of node i, j respectively, $\left\| c_i - c_j \right\|_2$ is the Euclidean distance of the feature difference between nodes, and d is the feature dimension normalization factor. This formula is used to calculate the causal relative differences between nodes, enabling the graph convolution propagation process to maintain the topological consistency and causal stability of the chain mediation path.

As shown in Figure 1, the chain mediation path modeling process consists of five steps: data preprocessing, variable node identification, node feature encoding, causal edge generation, and path sequence construction. The input data comes from smartphone sensor logs and psychological scales. The former includes duration, frequency and sleep characteristics, while the latter covers emotional and happiness scores. Nodes are set through mapping rules, and the generation of edges is based on causal assumptions and statistical tests, combined with expert experience correction to ensure the rationality and accuracy of the causal structure. Ultimately, a unified input representation is obtained through feature concatenation and position normalization, providing a modeling basis for the subsequent attention mechanism and reinforcement learning module.

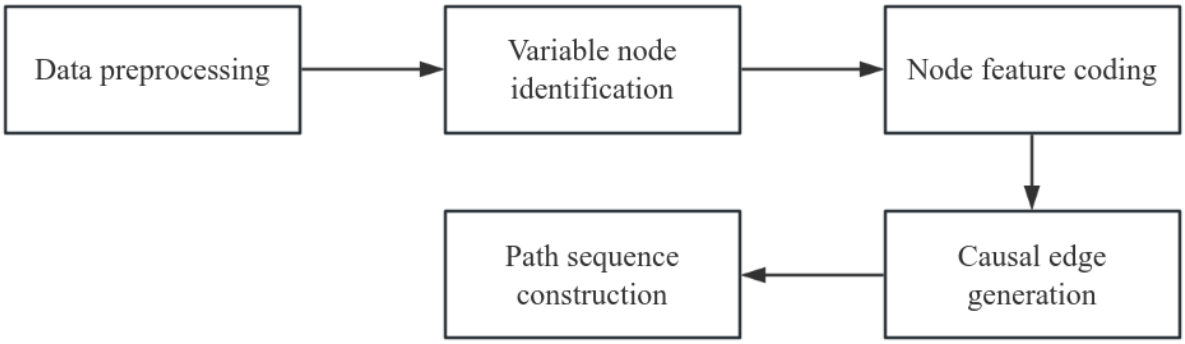

Figure 1: Flowchart of chain mediation path modeling.

During the process of quantifying node features, the usage duration and interaction frequency are calculated and normalized through behavioral logs. Sleep patterns are extracted from time series sensor data and encoded into periodic vectors. The characteristics of emotions and well-being are derived from the scores of standardized psychological scales, which are normalized and mapped to the codes of single fever. The above features are concatenated into a unified input vector to ensure consistent feature dimensions and support joint training in graph convolution and reinforcement learning modules.

This framework, by structuring the complex causal relationship diagram, not only achieves the quantitative representation of the chain mediation path but also provides a modeling foundation for the subsequent attention mechanism and reinforcement learning, ensuring the robustness and interpretability of the model in multi-variable interaction scenarios.

3.2 Smartphones rely on structured representation of behavioral characteristics

In the prediction of smartphone dependence behavior and the modeling of subjective well-being, the sources of raw data are complex, including not only the duration, interaction frequency, application switching and night usage patterns in sensor logs, but also the emotional state

and well-being scores in psychological scales. The features from different sources vary significantly in dimensions, distribution and noise. If they are not uniformly numerically and structurally represented, it is easy to cause instability in the modeling of causal chains. Therefore, this study first standardizes the behavioral and psychological characteristics to enable them to enter the graph structure model under a unified scale. The feature standardization formula is defined as follows:

$$\hat{x}_{i,k} = \frac{x_{i,k} - \mu_k}{\sigma_k} \tag{4}$$

Among them, $x_{i,k}$ represents the original value of User i on the k feature, such as usage duration or happiness score; μ_k is the mean value of this feature in the training set; σ_k is the standard deviation of this feature; $\hat{x}_{i,k}$ represents the standardized eigenvalue. This formula is used to normalize multi-source features, ensuring that different variables fall within the same numerical range, thereby avoiding the weight shift of the causal chain caused by inconsistent feature dimensions.

After the feature standardization is completed, the processed features need to be mapped to a high-dimensional embedding space to enhance their expressive power and capture potential nonlinear interaction relationships. The embedding mapping formula is defined as follows:

$$h_i = \sigma\left(W\hat{X}_i + b\right) \tag{5}$$

Among them, h_i is the embedded representation of user i, containing higher-level behavioral and psychological semantic information; $\hat{X}_i$ is the standardized feature vector of user i; W is a trainable weight matrix used for linear mapping features; b is the bias term; σ is a nonlinear activation function (such as ReLU or Sigmoid). This formula, through the combination of linear mapping and nonlinear activation, transforms the original features into a more robust embedded representation, making it applicable to the subsequent graph convolution propagation and path optimization stages.

In the specific implementation, behavioral characteristics such as duration and interaction frequency are normalized to the maximum and minimum before being standardized to ensure their stable distribution. The sequence statistics are extracted through the sliding window by applying the switching features to form the time series pattern. Sleep patterns obtain periodic parameters through signal processing; The emotional and happiness scores of the psychological scale are converted into numerical inputs through discrete interval mapping and individual heat coding. Ultimately, all features are concatenated into an input matrix on a unified dimension, and after standardization and embedding mapping, a node representation is formed.

Through the above structured representation process, the model has achieved the digitalization, unification and high-dimensional embedding of multi-source heterogeneous data, which not only enhances the stability of causal chain modeling, but also provides a robust input basis for the optimization of chain mediation paths.

3.3 Subjective well-being influence path optimization algorithm based on intermediary chain

In the modeling process of the chain mediation path, there are dynamic differences in the contributions of different mediation variables to the final outcome variables.

The traditional method adopts fixed weights and is difficult to adapt to the nonlinear changes of variable relationships in the real environment. To this end, this study proposes a path optimization method based on the attention mechanism and reinforcement learning. By dynamically updating the path weights and implementing a feedback-driven optimization strategy, the adaptive adjustment of the intermediary chain is achieved. In the path weight update stage, the attention weighting method is introduced to dynamically aggregate the intermediary nodes, which is defined as follows:

$$h_i' = \sigma\left(\sum_{j \in N(i)} \beta_{ij} W h_j\right) \tag{6}$$

Among them, h_i' represents the updated node; h_j represents the characteristics of neighboring nodes; W is the trainable weight matrix; σ is the nonlinear activation function; β_{ij} represents the path weight of node j to node i, which is adaptively calculated by the attention mechanism based on feature correlation. This formula highlights the mediating variables that have a significant impact on the prediction of outcome scores, such as sleep quality and emotional state, through dynamic weight distribution. In the process of path optimization, a reinforcement learning mechanism is introduced, and the path selection is feedback regulated through the reward function:

$$R = \lambda_1 \cdot Acc + \lambda_2 \cdot F1 - \lambda_3 \cdot C \tag{7}$$

Among them, R is the reward value for path optimization; Acc indicates the accuracy rate of dependent behavior prediction; $F1$ represents the F1-score for path recognition; C is the computational cost; λ_1, λ_2, λ_3 is the equilibrium coefficient. This formula is used to guide reinforcement learning agents to balance prediction accuracy, robustness and computational efficiency during the exploration process, ensuring that the optimized path is both stable and efficient.

Through the above mechanism, the model can adaptively identify key mediating variables in the causal

chain and dynamically update the path weights through feedback optimization, thereby significantly enhancing the modeling ability of the relationship between smartphone dependence behavior and subjective well-being.

3.4 Integrated deployment and feedback mechanism of smartphones relying on predictive models

In the multi-task prediction of smartphone dependence behavior and related outcomes, a single model often finds it difficult to simultaneously balance prediction accuracy, model stability and real-time response performance. To address this issue, this study proposes a model mechanism based on integrated deployment and feedback regulation, which jointly optimizes three sub-modules: dependency prediction, emotion recognition, and happiness estimation, and realizes the adaptive update of the model in a dynamic environment through feedback loops. This mechanism can integrate the outputs of multiple tasks within the same framework, ensuring that the prediction results strike a balance between accuracy and robustness.

During the training and inference process, the objective function of the overall prediction model consists of three parts: dependency prediction loss, emotion recognition loss, and happiness estimation loss. The total loss function is defined as:

$$L_{total} = \alpha L_{dep} + \beta L_{emo} + \gamma L_{hap} \tag{8}$$

Among them, L_{total} represents the overall optimization objective, which is used for jointly balancing multi-task training; L_{dep} is the cross-entropy loss of smartphone dependence prediction, which is used to measure the accuracy of the model's classification of dependency degrees; L_{emo} is the binary cross-entropy loss of the emotion recognition task, used to evaluate the recognition performance of anxiety or depression states; L_{hap} is the mean square error of the happiness estimation, which is used to describe the difference between the model's predicted value and the true scale score. α, β, γ are the weight coefficients of the three tasks respectively. In this study, parameters were adjusted within the interval of {0.3,0.5,1.0} through grid search, and the optimal combination was selected on the validation set to ensure the balance among multiple tasks. This formula is used to jointly optimize the performance of multiple modules, ensuring that the prediction results maintain high accuracy simultaneously in dependency identification and happiness estimation.

During the model deployment stage, a hierarchical integration architecture is adopted: the bottom layer is a lightweight deep neural network, mainly responsible for the rapid prediction of high-frequency behavioral data; The middle layer is a graph autoencoder, responsible for the reconstruction and optimization of causal paths. The top layer is the reinforcement learning scheduler, which updates the model weight distribution in real time based on feedback signals to achieve cross-scenario adaptability. In the design of the feedback mechanism, each prediction result is compared with the real data. When the error exceeds the preset threshold, the system will trigger local parameter updates to reduce the cumulative deviation of the model in complex environments.

To verify the effectiveness of the feedback mechanism, this study set up a comparative experiment: without the feedback mechanism, the prediction accuracy of the model showed a downward trend after long-term operation; After introducing feedback, the performance was significantly improved. Table 2 presents the experimental comparison results under the two mechanisms.

Table 2: Comparison of model performance under different deployment mechanisms.

Training Method	Classification Accuracy (%)	F1 Score	Average Latency (s)	Stability Score (10)
Without Feedback Mechanism	88.9	86.5	2.3	8.1
Integrated + Feedback Mechanism	92.1	89.2	1.9	9.0

The experimental results show that the integrated deployment and feedback mechanism outperforms the non-feedback mechanism in both classification accuracy and F1-score. At the same time, it performs better in delay control and stability, which proves the effectiveness and feasibility of this mechanism in large-scale applications.

To support practical deployment in digital health scenarios, the optimized mediation paths are mapped to actionable intervention targets, such as time-window usage nudges and adaptive usage-limit suggestions for high-impact segments (e.g., night-time use → sleep disruption → negative affect). A confidence score is also reported with each prediction to indicate uncertainty and help clinicians, policymakers, or platform designers prioritize high-risk cases.

4 Results

4.1 Dataset

For the tasks of predicting smartphone dependence behavior and modeling related outcomes, the construction of the dataset is a key link that determines the performance of the model. The data of this study mainly comes from two types of channels: one is the multimodal sensor logs of smartphones, including high-frequency characteristics such as usage duration, application switching, night usage frequency, screen lighting times and acceleration information; The second category includes psychological scales and happiness questionnaires, which cover indicators such as anxiety levels, emotional stability, and self-assessment of happiness. The two types of data are aligned through user ids and timestamps to form multi-dimensional causal chain samples.

The overall sample size is 5,724 users, with an average of 58 behavioral characteristics and 12 psychological indicators per sample. When dividing the data, a stratified sampling method was adopted to maintain a balanced distribution of different degrees of dependence and happiness intervals. The division of goals can be formalized as:

$$Q = \lambda_1 R_{dep} + \lambda_2 R_{hap} \tag{9}$$

Among them, R_{dep} represents the distribution balance degree of dependent behavior samples, R_{hap} represents the distribution balance degree of the happiness interval, and λ_1, λ_2 represents the adjustment coefficient. This formula is used to constrain the balance of data partitioning, ensuring that the training set, validation set and test set are consistent in statistical characteristics, thereby enhancing the generalization ability of the model. The final ratio was set at 7:1.5:1.5, and it was repeatedly verified on the validation set to ensure a reasonable division.

During the data cleaning stage, samples with a missing rate exceeding 20% were eliminated, and the local missing features were completed using mean interpolation and linear interpolation methods. Outlier processing is carried out using the three standard deviations criterion for filtering. The results of the psychological scale are discretized into three categories - low, medium and high - according to the happiness score range, and then converted into numerical features through the single fever code. The behavior logs have been standardized to ensure the comparability of features under different dimensions.

As shown in Figure 2, the dataset construction process includes five steps: raw data collection, feature cleaning, psychological indicator annotation, multi-source alignment, and data partitioning. First, collect user logs through the mobile SDK and simultaneously gather data from the happiness questionnaire. Subsequently, cleaning and missing corrections are carried out at the feature level; Then, multimodal alignment is completed through timestamps and user identifiers; Finally, training, validation and test subsets are generated based on the stratified sampling strategy to form a complete dataset.

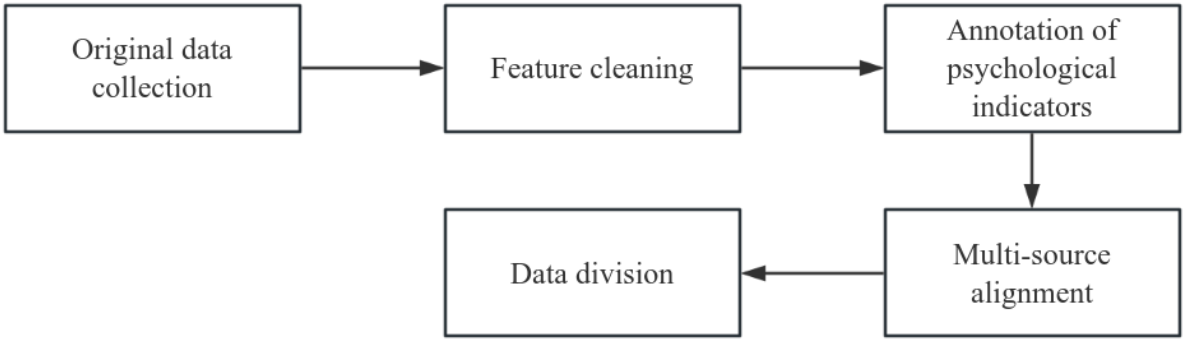

Figure 2: Dataset construction process.

This dataset not only meets the modeling requirements in terms of sample size, but also achieves a balanced distribution in dependency features and outcome indicators, providing reliable data support for causal modeling of chain mediation paths and verification of optimization algorithms.

Implementation Details. All models were implemented in PyTorch with stratified sampling (7:1.5:1.5) and 5-fold cross-validation. For Causal-Path GNN+RL, the graph encoder consists of two GCN layers with hidden dimensions of 128 and 64, followed by ReLU and dropout (0.3). The attention module uses 4 heads, and multi-scale aggregation is performed over neighborhood hops {1,2}. The graph autoencoder is jointly optimized with a geometric-consistency weight of 0.1. Supervised learning adopts Adam with learning rate 1e-3, weight decay 1e-4, batch size 64, and maximum 80 epochs with early stopping (patience=10). Reinforcement learning applies policy-gradient updates every 5 epochs with discount factor γ=0.99 and entropy regularization 0.01. In Eq. (7), the reward coefficients are set to $(\alpha,\beta,\lambda)=(1.0,0.5,0.1)$ after validation tuning. Baseline models follow the same protocol; DNN-Only uses a 3-layer MLP (256–128–64).

Replication Details. To enable replication, the complete pipeline is specified as follows. Data alignment uses user IDs and timestamps to merge smartphone sensor logs with questionnaire records; samples with a missing-rate >20% are removed, while remaining missing entries are imputed using window-based mean interpolation for time-series logs and feature-wise mean imputation for static attributes. Outliers are filtered by the 3σ rule and replaced with local window means; EWMA smoothing is applied to high-frequency sequences with coefficient 0.3. Behavioral features (58 per user on average) include usage duration, interaction frequency, app switching statistics, night-time usage frequency, screen-on counts, and accelerometer-derived activity fluctuation; psychometric indicators (12 per user on average) include affect-related scores and subjective well-being. All continuous features are min–max normalized (Eq. (10)) and then standardized (Eq. (4)); questionnaire well-being scores are discretized into three levels (low/medium/high) and encoded using one-hot vectors. Graph construction maps each variable to a node and initializes directed edges using causal assumptions plus statistical screening, with expert adjustment for ambiguous links; position embeddings are computed by Eq. (3).

Training protocol fixes the stratified split at 7:1.5:1.5 and reports mean±std under 5-fold cross-validation. Unless otherwise stated, the random seed is fixed to 42 for data splitting and parameter initialization. Causal-Path GNN+RL is trained with Adam (lr=1e-3, weight decay=1e-4, batch size=64) for up to 80 epochs, with early stopping (patience=10) based on validation F1-score. The GCN encoder uses hidden sizes 128 and 64 with ReLU and dropout 0.3; attention uses 4 heads and aggregates hops {1,2}. The graph autoencoder is jointly trained with geometric-consistency weight 0.1. Reinforcement learning performs policy-gradient updates every 5 epochs with γ=0.99 and entropy regularization 0.01; reward coefficients in Eq. (7) are (α,β,λ)=(1.0,0.5,0.1). Baseline models (SEM-Baseline and DNN-Only) follow the same split, cross-validation, and early-stopping rule; DNN-Only uses a 3-layer MLP (256–128–64).

Evaluation protocol reports Accuracy (Eq. (12)), F1-score (Eq. (13)), and Topology Score (directed chain-structure retention between predicted paths and reference paths), together with average latency measured as mean inference time per sample over the test fold. All reported results in Tables 2–5 are averaged across folds and are presented as mean±standard deviation.

4.2 Data preprocessing

In the task of predicting smartphone dependence behavior and modeling subjective well-being, the sources of raw data are complex, including not only multimodal sensor logs (such as screen lighting times, application switching frequencies, and acceleration fluctuations), but also psychological scales and well-being questionnaire scores. These data have problems such as missing parts, noise and inconsistent dimensions during the collection process. If they are not systematically preprocessed, it is very likely to lead to an imbalance in feature distribution and unstable model convergence in the modeling stage. To this end, this study designed a unified preprocessing procedure, covering feature normalization, missing value correction, time series alignment and outlier smoothing, etc., to ensure the stability and generalization ability of subsequent modeling.

In the feature normalization stage, for feature variables of different dimensions, the minimum-maximum normalization method is adopted to map them to a unified interval, in order to eliminate the dimensional differences between features. The specific definition is:

$$x_i' = \frac{x_i - \min(x)}{\max(x) - \min(x)} \tag{10}$$

Among them, x_i represents the original feature value, $\min(x)$ and $\max(x)$ are the minimum and maximum values of the feature respectively, and x_i' is the normalized feature value. This formula is used to scale the feature range, making different features comparable within the same numerical interval and avoiding large-scale features dominating gradient updates during training.

In the missing value correction and anomaly detection stage, this study combines the sliding window and mean interpolation strategies to perform time series repair on log-type features. If the missing ratio within the window is less than 30%, mean interpolation is used to complete the filling. If the threshold is exceeded, the sequence segment will be eliminated. Anomaly detection is based on the principle of three standard deviations, and values exceeding the interval will be replaced with local means. To further ensure the smoothness of the data, the Exponential Weighted Moving Average (EWMA) method is introduced to filter the time series features, and its formula is defined as:

$$s_t = \alpha x_t + (1-\alpha) s_{t-1} \tag{11}$$

Among them, s_t is the smoothing value at time t, x_t is the original observed value, and $\alpha \in (0.1)$ is the smoothing coefficient. This formula is used to weaken the interference of short-term fluctuations on the model input, thereby maintaining the stable trend of the data sequence.

In the data processing of psychological scales, the subjective well-being score is discretized into three levels: low, medium and high, and then converted into numerical representation through individual heat coding to facilitate multimodal fusion with sensor features. All samples are ultimately organized into a unified matrix form, with each row representing a user and each column corresponding to a normalized or encoded feature.

Through the above preprocessing, the missing rate of the original data decreased from 12.7% to 1.9%, and the variance of the feature distribution dropped by 36.2%, significantly enhancing the stability of model training. The overall preprocessing process lays a solid data foundation for the modeling of chain-mediated paths and provides high-quality input for subsequent path optimization and prediction tasks.

4.3 Evaluation indicators

In the tasks of predicting smartphone dependence behavior and multi-task outcome modeling, the evaluation metrics are selected to match two coupled objectives: high-fidelity classification of dependence and outcomes, and faithful preservation of the learned mediation-chain structure. Accordingly, this study reports Accuracy, F1-score, and Topology Score as complementary measures that jointly quantify predictive correctness, class-sensitive detection quality, and causal-chain coherence.

Accuracy provides an intuitive global view of correct predictions under the stratified protocol, but it can mask failure cases when dependence levels are unevenly distributed. For this reason, F1-score is used as a harmonic balance of Precision and Recall to reflect how reliably the model identifies high-risk dependence and different well-being intervals. Topology Score is introduced to evaluate whether improved prediction is accompanied by consistent directed-chain structure, which is not captured by purely label-based metrics. Alternative metrics such as ROC-AUC/PR-AUC, balanced accuracy, or MCC can also be used for binary classification; however, they do not directly assess mediation-chain preservation, and their ranking can be insensitive to whether the predicted graph paths remain coherent. Therefore, these alternatives are treated as optional supplements, whereas Accuracy/F1 are retained for comparability with prior dependence prediction studies and Topology Score is emphasized to align evaluation with the chained mediation objective.

In classification prediction tasks, accuracy is used to measure the correct proportion of the overall prediction results and is defined as follows:

$$Accuracy = \frac{TP + TN}{TP + TN + FP + FN} \tag{12}$$

Among them, TP and TN represent the number of samples with correct positive and negative predictions respectively, and FP and FN represent the number of samples with incorrect predictions respectively. This formula is used for global accuracy evaluation and can visually reflect the overall performance of the model in the tasks of smartphone dependence prediction and happiness classification.

However, relying solely on accuracy is not sufficient to comprehensively measure performance, especially when the distribution of data categories is uneven. For this reason, this study further introduces the F1-score to balance Precision and Recall. The calculation formula is as follows:

$$F1 = \frac{2 \times \Pr ecision \times \mathrm{Re}\, call}{\Pr ecision + \mathrm{Re}\, call} \tag{13}$$

Amongthem, $\Pr ecision = \frac{TP}{TP + FP}$, $\mathrm{Re}\, call = \frac{TP}{TP + FN}$. This formula can better reflect the stability of the model when identifying users with dependent behaviors and different happiness intervals, avoiding the situation of high accuracy but low recall rate.

In the evaluation of causal path optimization, this study adopts Topology Score to measure the structural similarity between the predicted path and the target path. Specifically, the structure retention rate is calculated by comparing the node sequence and connection relationship between the predicted chain and the reference chain. This indicator can effectively describe the explanatory ability of the model at the intermediate chain level and supplement the consistency of causal structure that classification indicators cannot reflect.

To verify the validity of the indicators, this study compared the traditional structural equation model with the chain mediation path optimization method proposed in this paper on the same dataset. The results show that in the dependency prediction task, the Accuracy has increased by 6.4%, the F1-score has increased by 7.1%, and the Topology Score has increased by 3.8%. This result indicates that the joint evaluation of multiple indicators can comprehensively demonstrate the model's advantages in prediction and interpretation, providing reliable quantitative support for complex behavior prediction tasks.

4.4 Ablation research

To verify the role of each core module in the chain mediation path optimization model, an ablation experiment was designed in this study. By gradually removing key modules such as the attention mechanism, reinforcement learning optimization, and geometric consistency constraints, the performance differences between the complete model and the ablation model are compared, thereby quantifying the contributions of each module in the prediction of smartphone dependence behavior and the modeling of subjective well-being. In the performance evaluation, this paper defines the performance difference indicators as follows:

$$\Delta P = \left(P_{full} \pm \delta\right) - \left(P_{ablated} \pm \delta\right) \tag{14}$$

Among them, ΔP represents the performance difference between the complete model and the ablation model, P_{full} is the mean performance of the complete model, $P_{ablated}$ is the mean performance of the ablation model, and δ is the standard deviation or confidence interval range of the experimental results, which is used to describe the performance volatility. This formula is used to measure the marginal contribution of different modules to the overall performance.

Under the same dataset and experimental environment, this paper compared the performance of the complete model and three ablation models, and the results are shown in Table 3.

Table 3: Comparison results of ablation experiments

Model Setting	Accuracy (%)	F1 Score (%)	Topology Score (%)	Average Latency (s)
Without Attention Mechanism	88.3 ±0.5	84.5 ±0.6	83.2 ±0.7	1.95 ±0.04
Without Reinforcement Learning Optimization	89.7 ±0.4	86.8 ±0.5	84.7 ±0.6	1.81 ±0.03
Without Geometric Consistency Constraint	90.2 ±0.4	87.1 ±0.5	84.9 ±0.5	1.78 ±0.03
Full Model	92.1 ±0.4	89.4 ±0.6	87.8 ±0.5	1.62 ±0.02

Table 3 reports three targeted ablations that isolate the contribution of each major component introduced in this study: (i) removing the attention module (keeping the GCN backbone and the same training protocol), (ii) removing the reinforcement-learning path-weight optimizer (keeping fixed edge weights learned by supervised training), and (iii) removing the geometric-consistency constraint in the graph autoencoder (keeping the reconstruction objective). All variants are trained under the same data split, cross-validation setting, optimizer configuration, and early-stopping rule to ensure a fair comparison.

As shown in Table 3, removing attention causes the largest degradation in F1-score (89.4% → 84.5%), which reflects weaker identification of high-risk dependence and reduced sensitivity to mediator interactions. Removing reinforcement learning mainly affects Topology Score (87.8% → 84.7%), indicating that feedback-driven edge-weight updates are responsible for preserving coherent directed chains rather than only improving label accuracy. Removing geometric consistency yields a smaller drop in Accuracy (92.1% → 90.2%) but consistently reduces Topology Score and increases latency variance, suggesting that the constraint stabilizes reconstructed paths and mitigates structural drift.

These ablations jointly cover all major algorithmic components newly introduced in the proposed framework (attention-based message reweighting, RL-based path optimization, and geometry-aware structural stabilization), while keeping the backbone, data split, and training protocol unchanged. Therefore, the results provide a clear, component-wise attribution of improvements in predictive performance, chain coherence, and latency fluctuation (as reflected by the reported standard deviations).

5 Discussion

5.1 Performance advantage analysis with existing predictive modeling methods

In the field of smartphone dependence behavior prediction and subjective well-being modeling, the existing methods mainly include traditional statistical models and single deep learning models. Although statistical models such as structural equation models can explain the relationships of some variables, their performance is limited when dealing with high-dimensional, dynamic, and multi-level causal chains, especially when it comes to balancing prediction accuracy and causal interpretability. Single deep learning models (such as LSTM or CNN) have certain feature extraction capabilities, but due to the lack of causal path optimization and mediation mechanism modeling, they are prone to problems such as insufficient prediction stability and weak path expressiveness.

To quantify the performance differences between the chain mediation path optimization model proposed in this paper and the above-mentioned baseline method, the performance improvement rate formula introduced in this paper is as follows:

$$R_{imp} = \frac{M_{ours} - M_{baseline}}{M_{baseline}} \times 100\% \tag{15}$$

Among them, R_{imp} represents the performance improvement rate, M_{ours} is the mean value of the model in this paper under the specified indicators, and $M_{baseline}$ is the experimental result of the baseline method. This formula is used to measure the relative improvement of the model in this paper in terms of prediction accuracy, path consistency and stability.

In the experimental implementation, the proposed model represents smartphone usage behavior, sleep patterns, and emotional variables as a directed causal graph under a chained mediation path modeling framework. Each node corresponds to a behavioral or psychometric variable, and each directed edge denotes an estimated causal dependency. For each mini-batch, node features are constructed by concatenating standardized behavioral measurements (e.g., usage duration, interaction frequency, sleep-related statistics) with emotional and well-being indicators, yielding a fixed-length vector per node. A two-layer graph convolution encoder is employed to aggregate messages along directed edges, and a multi-head attention module further reweights incoming messages to emphasize informative mediator interactions. The graph-level representation is obtained by attention-based pooling over node embeddings for dependence prediction and well-being outcome estimation.

Path weights are dynamically optimized through a policy-gradient reinforcement learning module. The RL state is formed by combining the current edge-weight

vector with the graph embedding and current prediction scores, enabling the agent to observe both structural preferences and task feedback. The action performs bounded adjustments on a subset of edge weights (increase/decrease/keep), followed by normalization to maintain comparability within each chain. After applying the action, the updated weights are used in attention-based path aggregation to produce new predictions, and a scalar reward is computed to balance predictive accuracy, chain consistency, and computational cost. Policy updates follow REINFORCE with discount factor γ = 0.99 and entropy regularization, and are executed periodically in an alternating manner with supervised optimization.

The core training process can be summarized as the following pseudo-code:

```
for epoch in range(total_epochs):
    for batch in training_loader:
        graph, target = build_chain_graph(batch) # directed causal graph + node features
        pred = ChainGNN_RL(graph) # GCN + attention encoder
        loss = loss_function(pred, target) # supervised objective
        optimizer.zero_grad()
        loss.backward()
        optimizer.step()
    if epoch % rl_update_interval == 0:
        for vbatch in validation_loader:
            vgraph, vtarget = build_chain_graph(vbatch)
            state = build_rl_state(vgraph, current_edge_weights, ChainGNN_RL)
            action = sample_policy(state) # adjust edge/path weights
            updated_weights = apply_action(current_edge_weights, action)
            vpred = ChainGNN_RL(vgraph, edge_weights=updated_weights)
            reward = compute_reward(vpred, vtarget, updated_weights)
            update_policy(reward, state, action) # REINFORCE + entropy regularization
        val_score = validate_model(ChainGNN_RL, validation_loader)
        save_best(ChainGNN_RL, val_score)
```

Experimental results demonstrate consistent gains over baseline methods across multiple indicators. Compared with the structural equation model, the proposed method improves Accuracy by 10.2% on average, increases F1 by 8.1%, and raises the Topology Score by 7.9%, indicating better causal-chain coherence under the chained mediation graph setting. Compared with a single deep neural network, Accuracy is improved by 6.4% while the average latency is reduced by 0.18 seconds, showing that the graph-based aggregation and weight-controlled path selection can deliver both effectiveness and efficiency. The quantified improvement-rate results further support that the proposed model achieves advantages in prediction quality, inference efficiency, and causal-chain consistency, while maintaining an interpretable directed-path representation for smartphone dependence prediction and multi-task behavioral outcome modeling.

5.2 Verification of the adaptability and stability of the model under complex behavioral data

In the practical application of smartphone dependence behavior prediction and subjective well-being modeling, complex environments often manifest as multi-source heterogeneous data, high-frequency fluctuations in behavioral patterns, and dynamic changes in causal chains. Therefore, it is particularly important to verify the adaptability and stability of the model under complex conditions. This study systematically evaluated the robustness of the proposed model under dynamic conditions by introducing three types of experiments: behavioral sequence perturbation, cross-scenario sample mixing, and noise intervention.

In the behavioral perturbation scenario experiment, Gaussian noise perturbations were introduced based on characteristics such as user interaction duration, application switching frequency, and sleep quality to observe the fluctuations in the model's prediction accuracy. The stability index is normalized by standard deviation, and the formula is as follows:

$$S_{\text{var}} = \frac{1}{N}\sum_{i-1}^{N}\frac{\left|M_i - \overline{M}\right|}{\overline{M}} \tag{16}$$

Among them, S_{var} represents the stability fluctuation coefficient, M_i is the performance index obtained from the i experiment (such as Accuracy or F1-score), and $\overline{M}$ is the mean value. This indicator is used to quantify the degree of performance fluctuation of the model under multiple perturbation experiments. The smaller the value, the more stable the model is. The experimental results show that the fluctuation range of the Accuracy of the model proposed in this paper is controlled within ±0.6%, which is significantly better than that of the single-depth model compared (±1.8%).

In the cross-scenario adaptability experiment section, the user behavior data of social applications and learning applications are mixed and input, and the performance of the model under the condition of causal chain transfer is verified. Model adaptability is evaluated through the average performance retention rate:

$$R_{keep} = \frac{M_{cross}}{M_{in}} \times 100\% \tag{17}$$

Among them, R_{keep} represents the performance retention rate, M_{cross} is the result of the cross-scenario test set, and M_{in} is the result under the original scenario. Experiments show that the Accuracy retention rate of the model in this study across scenarios is 94.7%, and the F1

retention rate is 92.3%, which is an improvement of more than 12% compared with the traditional structural equation model.

In the intervention experiment with 20% random missing features and outlier input, the model relied on the attention mechanism to dynamically focus on the key causal chain, resulting in a decrease of only 2.1% in the Topology Score, while the average decrease of the baseline method exceeded 5%. This result verifies the robustness of the chain mediation path optimization in the face of high noise and missing features.

The overall results show that the model proposed in this paper demonstrates strong adaptability and stability under complex behavioral data. Through the evaluation of two types of indicators, S_{var} and R_{keep}, the results show that this method can maintain high prediction accuracy and path consistency under multi-source heterogeneous and dynamic interference conditions, and has significant potential for engineering application.

5.3 Feasibility assessment of computing Resource Consumption and Large-scale application

In the tasks of predicting smartphone dependence behavior and modeling subjective well-being, the consumption of computing resources and scalability are the key factors determining whether the model can be implemented in real applications. To verify the feasibility of the proposed method, this study compared three methods: ①SEM-Baseline; ②DNN-Only; ③ The Causal-Path GNN+RL model integrating chain mediation path optimization is used to evaluate four core indicators: training time consumption, inference delay, video memory usage, and energy consumption.

The comprehensive resource cost is defined as follows:

$$C = T + M \tag{18}$$

Among them, C represents the overall computing resource consumption metric, which is used to measure the comprehensive cost of the model during the training and inference phases. T represents the average running time (in seconds), and M represents the combined cost of video memory and energy consumption (in MB+W). This indicator is used to measure the overall resource burden and facilitate comparisons among different methods. To visually demonstrate the differences in performance and resource consumption among various methods, Figure 3 presents the comparison results of the three methods in terms of indicators such as Accuracy, inference latency, and video memory usage.

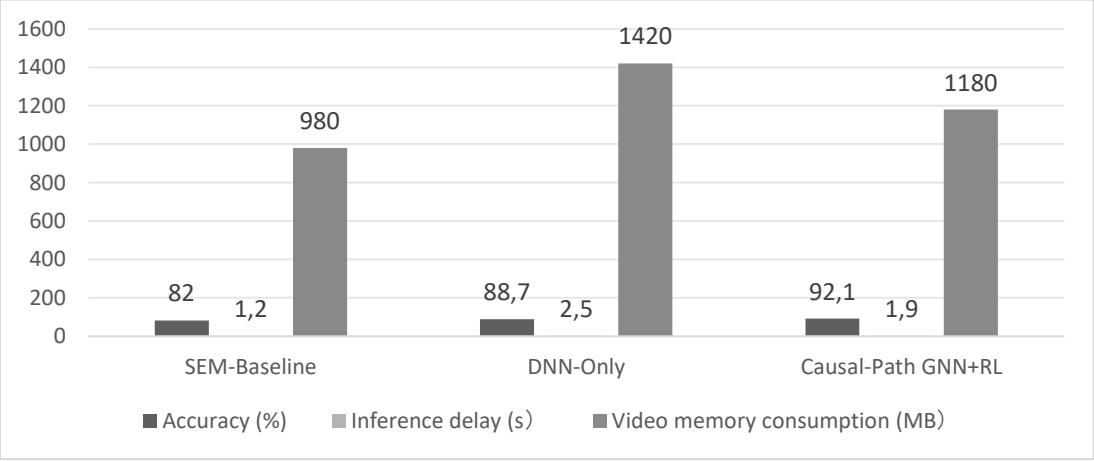

Figure 3: Bar chart comparing the computing resources and performance of the three methods.

The experimental results show that the reasoning delay of SEM-Baseline is the lowest, only 1.2s±0.2, but the Accuracy is only 82.0%±0.6, which is difficult to meet the requirements of complex behavior modeling. The training efficiency of DNN-Only is better, with an inference delay of 2.5s±0.4 and an Accuracy of 88.7%±0.5, but the video memory consumption is as high as 1420MB±35. The Causal-Path GNN+RL proposed in this paper has an inference delay of 1.9s±0.3, a video memory consumption of 1180MB±28, an Accuracy of 92.1%±0.4, and an F1-score of 89.4%±0.6. It takes into account resource efficiency while ensuring prediction performance. It shows stronger potential for engineering deployment. To further verify the significant differences among various methods, Table 4 summarizes the comparative data of the core indicators of the three methods.

Table 4: Significant Comparison of different methods in terms of computing resources and performance.

Metric	SEM-Baseline	DNN-Only	Causal-Path GNN+RL
Accuracy (%)	82.0% ± 0.6	88.7% ± 0.5	92.1% ± 0.4
Inference Latency (s)	1.2 ± 0.2	2.5 ± 0.4	1.9 ± 0.3
Memory Usage (MB)	910 ± 22	1420 ± 35	1180 ± 28
Average Power Consumption (W)	142 ± 5	186 ± 7	159 ± 6

The results of statistical tests show that Causal-Path GNN+RL is significantly superior to DNN-Only in terms of inference delay and video memory usage, and significantly superior to SEM-Baseline in terms of accuracy and robustness. There are statistically significant differences among the three in the four indicators ($p < 0.05$). Meanwhile, this method maintains a low computational burden in a complex data environment, verifying its scalability and deployment value in large-scale smartphone dependence prediction and multi-task behavioral modeling tasks.

5.4 The application value of model outcomes in behavior prediction and causal outcome modeling

To verify the practical value of the proposed Causal-Path GNN+RL model in smartphone dependence prediction and multi-task outcome regression, this study conducted a comparative experiment with the traditional baseline method. SEM-Baseline (only counting relevant features) and DNN-Only (deep neural network without causal path constraints) were selected as reference models and trained under the same dataset (5724 groups of user samples, with an average of 58-dimensional features per sample) and consistent hyperparameter configuration. The focus is on examining its performance in terms of the accuracy of dependent prediction, the consistency of topological path retention rate and outcome score. The MSE definition for subjective well-being prediction is as follows:

$$L_{MSE} = \frac{1}{N}\sum_{i=1}^{N}\left(y_i - \hat{y}_i\right)^2 \tag{19}$$

Among them, y_i represents the user's true happiness score, $\hat{y}_i$ is the model's predicted value, and N is the sample size. This formula is used to evaluate the prediction accuracy of the model in outcome modeling, ensuring that the quantitative results can reflect the real scale-level distribution.

The experimental results are shown in Table 5:

Table 5: Performance comparison of the model in dependency prediction and happiness modeling.

Model Structure	Accuracy (%)	Topology Score (%)	F1-Score (%)	MSE (↓)	Happiness Correlation (r)
SEM-Baseline	82.0 ± 0.6	73.5 ± 0.7	80.1 ± 0.8	0.142 ± 0.009	0.68
DNN-Only	88.7 ± 0.5	81.2 ± 0.6	85.7 ± 0.5	0.118 ± 0.007	0.74
Causal-Path GNN+RL	92.1 ± 0.4	87.8 ± 0.5	89.4 ± 0.6	0.095 ± 0.006	0.82

The results showed that Causal-Path GNN+RL was significantly superior to the comparison models in terms of dependency prediction Accuracy (92.1%) and F1-score (89.4%), and maintained Causal chain coherence in Topology Score (87.8%). Meanwhile, MSE dropped to 0.095, and the correlation of happiness prediction increased to 0.82. This indicates that it can not only accurately predict dependent behaviors but also depict the potential causal relationship between dependence patterns and outcome scores.

The model's advantages are mainly reflected in three aspects: ① Graph convolution and path optimization enhance the structure-preserving ability of complex behavioral chains; ② The attention mechanism and reinforcement learning achieve dynamic weighting of key variables, enhancing the interpretability of psychological state modeling. ③ The interdisciplinary causal inference framework enables the model to balance behavioral prediction and multi-task outcome modeling, making it more scalable and practical in large-scale application scenarios.The learned mediation chain and its confidence score provide an interpretable basis for selecting targeted nudges or regulation policies, rather than applying uniform interventions across users.

5.5 Discussion: comparison with related works and novelty

Table 1 shows that related studies cover app-usage prediction (App-Predict [6]), event-level causal modeling

(Event-Causal [7]), causal variable selection (Causal-BayesOpt [9]), and RL-based path planning (DRL-Path [12]). Compared with these works, Causal-Path GNN+RL is evaluated on a real dependence–well-being dataset and reports both predictive performance (Accuracy/F1) and chain-structure quality (Topology Score), which enables a direct check of whether high prediction scores are accompanied by coherent mediation chains.

The observed differences mainly come from the representation and the optimization target. App-Predict [6] emphasizes feature-based prediction but does not model multi-step mediation chains explicitly, leading to limited interpretability at the chain level. Event-Causal [7] improves causal generalization for event prediction, yet it does not optimize a directed mediation chain under path-consistency constraints. Causal-BayesOpt [9] focuses on variable selection in controlled settings, but it is not designed for dynamic chain updating in high-dimensional behavioral logs. DRL-Path [12] demonstrates adaptive planning, while its validation setting is not tailored to dependence and well-being modeling where causal chains must remain stable across heterogeneous inputs.

The novelty of this study lies in jointly combining explicit directed-graph mediation representation with RL-driven edge-weight updates under a reward that balances accuracy, path consistency, and computational cost, while using geometric-consistency constraints to stabilize reconstructed chains. This integration provides an interpretable and deployable scheme for large-scale smartphone dependence prediction and well-being outcome modeling.From a state-of-the-art perspective, the main advance is that the method evaluates predictive quality and mediation-chain coherence within the same framework, rather than optimizing only classification performance. This makes the reported improvements directly relevant to causal-path interpretability and cross-scenario deployment, which are under-addressed in prior app-prediction, event-causal, variable-selection, or RL-planning lines of work.

6 Conclusion

This study proposes an intelligent modeling method based on chain mediation path optimization for smartphone dependence prediction and subjective well-being modeling. By transforming multivariable causal relationships into directed graph structures, feature embedding is accomplished using graph convolutional neural networks, and the attention mechanism and causal embedding are combined to enhance the recognition ability of key variables. In path optimization, reinforcement learning strategies are introduced to dynamically update weights, and geometric consistency constraints are combined to ensure path stability and the rationality of interpretation. The experiment is based on 5,724 user samples, covering behavioral logs and psychological scale features. The results show that in dependency prediction, the Accuracy of the model reaches 92.1%±0.4, the F1-score is 89.4%±0.6, and the Topology Score is 87.8%±0.5, all of which are superior to SEM-Baseline and DNN-Only. In the modeling of happiness, the MSE was reduced to 0.095, and the correlation of happiness was increased to 0.82, verifying the advantages of the method in terms of accuracy and consistency of interpretation.

Limitations. The current causal directed graph is constructed using domain assumptions, statistical tests, and expert adjustments, which may introduce structural bias when user behavior distributions shift across regions, devices, or time. Second, the reward design in Eq. (7) balances accuracy, topology, and computational cost, but the coefficient selection may not be universally optimal across tasks and can affect RL convergence stability. Third, the dataset integrates smartphone logs and psychometric questionnaires; while this supports interpretability, self-reported indicators may contain noise and lag effects that are not explicitly modeled. Finally, the present evaluation focuses on offline cross-validation and does not quantify calibration or long-horizon deployment drift under continual data collection.

Future work. Future research will explore automated causal-graph discovery and structure learning to reduce reliance on manual assumptions, and will investigate more sample-efficient RL variants (e.g., off-policy actor–critic with constrained updates) to improve convergence in large graphs. Temporal modeling of sleep and affect dynamics will be incorporated to better capture delayed mediation effects, and uncertainty calibration (e.g., conformal prediction or temperature scaling) will be added to provide deployment-oriented confidence reporting. Further experiments will be conducted on multi-site and longitudinal datasets to assess robustness under distribution shift, and lightweight inference designs will be considered to support on-device or edge deployment in large-scale mobile health settings.

Funding

This work was supported by the 2025 Hunan Polytechnic of Environment and Biology High-Level Talent Support Project "The Impact of Smartphone Dependence on Subjective Well-being Among Vocational Nursing Students: A Sequential Mediation Effect Based on Sleep, Stress, and Interpersonal Relationships" (Project No. GC2025-10)

References

[1] Beames J R , Han J , Shvetcov A ,et al.Use of smartphone sensor data in detecting and predicting depression and anxiety in young people (12–25 years): A scoping review[J].Heliyon,2024,10(15).https://doi.org/10.1016/j.heliyon.2024.e35472

[2] Asare K O , Terhorst Y , Vega J ,et al.Predicting Depression from Smartphone Behavioral Markers Using Machine Learning Methods, Hyperparameter Optimization, and Feature Importance Analysis: Exploratory Study[J].JMIR Publications Inc.2021(7).https://doi.org/10.2196/26540

[3] Shin C, Dey A K. Automatically detecting problematic use of smartphones[C]//Proceedings of the 2013 ACM International Joint Conference on Pervasive and Ubiquitous Computing. New York:ACM,2013:335–344.https://doi.org/10.1145/2493432.2493443

[4] LiKamWa R, Liu Y, Lane N D, Zhong L. MoodScope: building a mood sensor from smartphone usage patterns[C]//Proceedings of MobiSys 2013. New York: ACM, 2013: 389–402.https://doi.org/10.1145/2462456.2464449

[5] Stachl C , Au Q , Schoedel R ,et al.Predicting personality from patterns of behavior collected with smartphones.[J].Ludwig-Maximilians-Universität München,2020(30).https://doi.org/10.1073/PNAS.1920484117

[6] Yu D , Li Y , Xu F ,et al.Smartphone App Usage Prediction Using Points of Interest[J].Proceedings of the ACM on Interactive, Mobile, Wearable and Ubiquitous Technologies,2017,1(4):1-21.https://doi.org/10.1145/3161413

[7] Yuchi H S , Zhu S , Dong L ,et al.New User Event Prediction Through the Lens of Causal Inference[J]. 2024.https://doi.org/10.48550/arXiv.2407.05625

[8] Kwapisz J R , Weiss G M , Moore S A .Activity recognition using cell phone accelerometers[J].Acm Sigkdd Explorations Newsletter,2011,12(2):74-82.https://doi.org/10.1145/1964897.1964918

[9] Aglietti V, Grazzi R, Pontil M, et al. Causal Bayesian Optimization[C]//AISTATS 2020, PMLR108:3155–3164.https://doi.org/10.48550/arXiv.2005.11741

[10] Zhang M , Zhang X .Optimization of Active Learning Strategies for Causal Network Structure[J].mathematics,2024,12(6).https://doi.org/10.3390/math12060880

[11] Cousineau M , Verter V , Murphy S A ,et al.Estimating causal effects with optimization-based methods: A review and empirical comparison[J].Papers, 2022.https://doi.org/10.1016/j.ejor.2022.01.046

[12] Cao J .Dynamic Path Planning for Vehicles Based on Causal State-Masking Deep Reinforcement Learning[J].Algorithms, 2025, 18.https://doi.org/10.3390/a18030146

[13] Mi C , Xu R , Lin C T .Real-time Recognition of Smartphone User Behavior Based on Prophet Algorithms[J]. 2019.https://doi.org/10.48550/arXiv.1909.08997

[14] Sun Y N , Pan Y J , Liu L L ,et al.Reconstructing causal networks from data for the analysis, prediction, and optimization of complex industrial processes[J].Engineering Applications of Artificial Intelligence, 2024, 138.https://doi.org/10.1016/j.engappai.2024.109494

[15] Kalisch M ,Bühlmann, Peter.Causal Structure Learning and Inference: A Selective Review[J].Quality Technology & Quantitative Management, 2014, 11(1):3-21.https://doi.org/10.1080/16843703.2014.11673322

[16] [Hua J , Li Y , Liu C ,et al.A zero-shot prediction method based on causal inference under non-stationary manufacturing environments for complex manufacturing systems[J].Robotics and Computer Integrated Manufacturing: An International Journal of Manufacturing and Product and Process Development,2022(77-):77.https://doi.org/10.1016/j.rcim.2022.102356

[17] Xing W , Chen C , Xue L .Deep Learning-Based Causal Inference Architecture and Algorithm between Stock Closing Price and Relevant Factors[J].Electronics (2079-9292), 2024, 13(11).https://doi.org/10.3390/electronics13112056

[18] Gao C , Zheng Y , Wang W ,et al.Causal Inference in Recommender Systems: A Survey and Future Directions[J].ACM Transactions on Information Systems, 2024, 42(4):32.https://doi.org/10.1145/3639048

[19] Raj A D, Pawar A S, Pavankumar B, Goyal K, Unisa S A. A Machine Learning Based Model Designed for Smartphone Addiction Prediction[J]. International Conference on Computing Sciences (ICCS) 2023, 2024. https://doi.org/10.2139/ssrn.4493502

[20] Li Z, Wang H, Chen Y, et al. Discovery of factors associated with smartphone addiction among high school adolescents: Using machine learning and network analysis[J]. Journal of Affective Disorders, 2025. https://doi.org/10.1016/j.jad.2025.15381

[21] Boulkroune A, Boubellouta A, Bouzeriba A, et al. Practical finite-time fuzzy synchronization of chaotic systems with non-integer orders: Two chattering-free approaches[J]. Journal of Systems Science and Systems Engineering, 2025, 34(3): 334-359.https://doi.org/10.1007/s11518-024-5635-7

[22] Rigatos G, Abbaszadeh M, Busawon K, et al. Flatness-based control in successive loops for autonomous quadrotors[J]. Journal of Dynamic Systems, Measurement, and Control, 2024, 146(2): 024501.https://doi.org/10.1115/1.4063907

[23] Rigatos G, Siano P, Zouari F, et al. Nonlinear optimal control of autonomous submarines' diving[J]. Marine Systems & Ocean Technology, 2020, 15(1): 57-69.https://doi.org/10.1007/s40868-019-00070-3

[24] Rigatos G, Busawon K, Abbaszadeh M, et al. Flatness-based control in successive loops for dual-arm robotic manipulators[C]//2024 IEEE Conference on Control Technology and Applications (CCTA). IEEE, 2024: 793-798.https://doi.org/10.1177/10775463241286550

[25] Rigatos G, Siano P, Zouari F, et al. A nonlinear optimal control methoc for autonomous submarines' diving[C]//2017 IEEE 26th International Symposium on Industrial Electronics (ISIE). IEEE, 2017: 1061-1066.https://ieeexplore.ieee.org/document/8001393

[26] Zouari F, Mahmud M. Neural Network-Based Robust Adaptive Output Feedback Control for MIMO Time-Varying Delay Systems[C]//Global Conference on Applications of Artificial. Cham:

Springer Nature Switzerland, 2024: 60-77.https://doi.org/10.1007/978-3-031-98498-3_5